GEOLOGICAL INVESTIGATION ON THE SPECTRAL UNITS OF PHOBOS AND DEIMOS. H. Kikuchi[1], H. Miyamoto[1], R. Hemmi[1], [1]Department of System Innovation, School of Engineering, The University of Tokyo, Japan. (kikuchi@seed.um.u-tokyo.ac.jp)

Introduction: The appearance of the Martian satellites, Phobos and Deimos, differ from one another, in spite of some similarities: impact cratering, orbital inclination, orbital eccentricity, low gravity, and thermal cycling. Comparing the two satellites with similar environments is important for understanding the origins and the evolutionary histories. The surface of Phobos is spectrally divided into two units: red and blue [1, 2]. The spectral slope of the red unit is steeper than that of the blue unit near-infrared spectrum by OMEGA and GRISM imaging spectrometers [3]. On the other hand, the high resolved spectral data of Deimos is obtained by CRISM. In order to the resolution, about 1200 m/pixel, the global spectral feature, which is similar to the red unit on Phobos is only obtained. However, the surface of Deimos could be divided into the two units by the calibrated data in the three HiRISE colours [4]. Although these false-colour images are insufficient to identify materials, they are clues to understand the evolutionary history of the surface. Because they are as high resolution as image data, we can link to the geological morphologies and consider the geological history. In this study, we examined the surfaces of both satellites in detail for each unit.

Crater counting on red and blue regions: To define the red and blue regions on Phobos, we used the color map, which is released by MExLab web-site in (http://mexlab.miigaik.ru/eng/). The data is based on HRSC color channel images and have been calibrated radiometrically and positionally [6, 8]. Using this map, we delineated the four study regions around Stickney crater (Fig. 1): Blue East, Blue South, Red Inside, and Red East. The surface area is 63.5, 71.3, 26.7, and 42.7 km^2 respectively. In order to measure the diameters and locations of the impact craters, we used the Small Body Mapping Tool (SBMT) [5]. This tool determines the central coordinate and diameter of craters, when three points are selected along the crater rim on the Stooke maps [6] rendering on the Gaskell shape model [7]. The resolution of our study regions ranged from 6 to 20 m/pixel. As a result, on the surface of Phobos, totally 3276 craters were identified: 1533 craters in Red East, 216 craters in Red Inside, 529 craters in Blue South, and 998 craters in Blue East around Stickney crater. Considering resolutions of each area, 950 craters over 30 m in Red East, 88 craters over 100 m in Red Inside, 249 craters over 100 m in Blue South, 489 craters over 50 m in Blue East were selected.

On craters with D < 400 m, no significant difference in crater density was detected among the four regions on Phobos. On the other hand, on craters with D > 400m on Phobos, the formation age of each area is Red East < Blue East < Blue South < Red Inside in the oldest order approximately.

On the surface of Deimos, For defining study Blue and Red unit area on Deimos, we used the calibrated Deimos data image data from ESP_012068_9000 [4]. Using this image, we defined two study area as Red, and Blue (Fig. 1). We rendered this image onto a shape model by Thomas [8], and measured each surface area: 20.3 and 26.4 km^2 respectively. For crater counting on Deimos, we rendered Stooke's map [6] onto the shape model. On study area, the image resolution is 14-20 m/pixel. As a result, on the surface of Deimos, 41 (Red), and 44 (Blue) craters were identified. No significant difference in crater density was detected between two units.

Comparing between the power law of crater size-frequency distributions (CSFD) of Phobos and that of Deimos, we found that the power law of CSFD of Phobos is steeper than that of Deimos. This tendency is consistent with previous study [9].

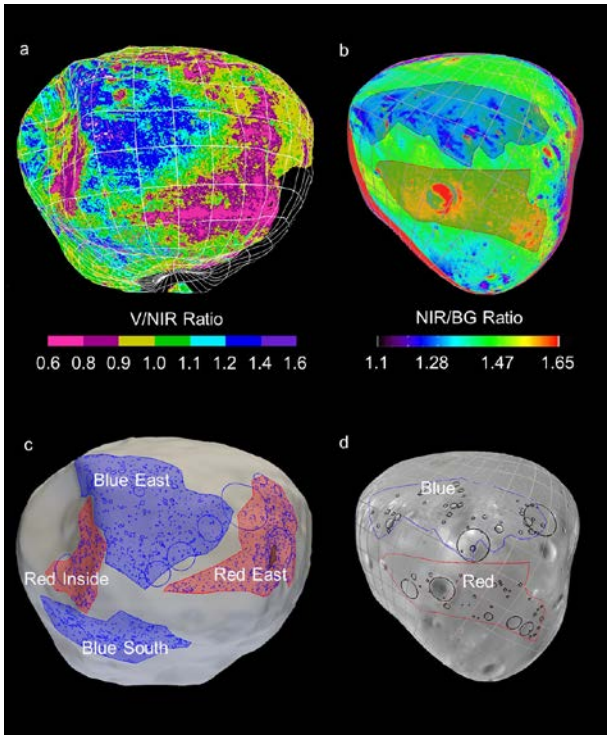

Figure 1. Spectral maps of Phobos (a) and Deimos (b) rendering on the shape models. The four study areas on Phobos (c) and the two study areas on Deimos (d) are outlined on the maps.

Dynamic height around Stickney crater: We investigate the topography around Stickney crater on Phobos. Its orbit is decaying due to the tidal force of Mars. This tidal force causes the gravity field of Phobos to spatially vary. Thus, in the previous studies, dynamic height was calculated taking this effect into account, and the topographic changing is well understood [8, 10]. Therefore, according to the calculation of this dynamic height, we investigate how the dynamic height in the vicinity of Stickney crater changes as a result of a change in the orbital distance in detail.

Data regarding the degree 2 gravity coefficients such as C_{20}, C_{22} of Phobos have not yet been constrained because spacecraft have not yet flown close enough to measure them at sufficient accuracy [11]. Previous studies calculated the self-gravity field of Phobos from the ellipsoidal or (more accurately) polyhedron shape model with the assumption of homogeneous inner structure. First, we calculate the self-gravity field, using polyhedron shape model. Because recent resolution of shape model is about 100 m/pixel, we divide the numerical shape model volumetrically into 1,602,854 small triangular pyramids of volume Δv, resulting in N = 57,148 surface triangles with a total of 285,448 vertices. Under the assumption of homogeneous bulk density value ρ, the self-gravity field on the surface can be calculated:

$$U = G\rho \sum_{i=1}^{N} \frac{\Delta v_i}{r_i}$$

where G is the gravitational constant, and r_i is the distance from the field point to the ith mass element.

Second, in order to calculate the potential energies per unit mass of the measured and reference points, Mars is considered as a point mass. The frame is Phobos-fixed rotating frame whose positive x-axis points to Mars. The positive y-axis points opposite to the orbital direction, and the positive z-axis is aligned with Phobos' rotation axis. Although Phobos has slight eccentricity e = 0.0151, we assume the value as zero. From tidal and centrifugal and self-gravitational forces, we calculate the Jacobi integral:

$$-J = \frac{n^2}{2}\left(x + R_P - \frac{m}{M}R_P\right)^2 + \frac{n^2 y^2}{2} + \frac{GM}{R} - U$$

where n is the mean motion of the orbit, m is the mass of Phobos, M is the mass of Mars, R_P is the semi-major axis of Phobos. Then, we calculate the dynamic height (H) defined as [12]. We adopt the same value of [13]: J_0 is 6.76 x 10^{-5} km^2/s^2, and g_0 is 8.4 x 10^{-6} km/s^2. Changing the distance between Phobos and Mars, Current distance, 3.25, 3.84, 4.43, 5.02, and 5.61 R_M, we calculate the dynamic height for each case.

As a result, the dynamic height of our result is good similar to ones of previous studies [10, 13]. From longitude 0° to 90° W and Latitude -45° to 45°, which is around Stickney crater, we found that the dynamic height of eastern rim of Stickney crater gets higher as the orbital distance between Phobos and Mars decrease. When R_P is greater or equal to 3.84 R_M, the dynamic height is largest on the east side of Stickney crater (Fig. 2).

Discussions and Implications: Given that the blue unit represents the characteristics of the surface material, an event where craters with D < 200 m were degraded would occur to the east side of Stickney on Phobos, because the crater density in this region is the smallest compared to all other regions. On the other hand, in both regions of the blue unit of Phobos to south side of Stickney and the blue unit on Deimos, the blue materials may be thinly deposited on each surface.

Furthermore, the result of crater counting on Phobos indicates that blue East and Blue South does not necessary to form same time. Because the dynamic height of the southwestern rim of Stickney crater is relatively low in all cases, the formation process of these two blue units in Phobos may be different.

References: [1] Murchie S. L. et al. (1991) *JGR, 96,* 5925-5945. [2] Murchie S. and Erard S. (1996) *Icarus, 123,* 63-86. [3] Fraeman A. et al. (2012) *JGR, 117,* E11. [4] Thomas N. et al. (2011) *PSS, 59,* 1281-1292. [5] Kahn E. et al. (2011) *LPS XLII,* Abstract #1618. [6] Stooke P. (2012) *Stooke Small Bodies Maps V2. 0. NASA Planetary Data System*. [7] Gaskell R.W. (2011) Gaskell Phobos Shape Model V1.0. VO1-SA-VISA/VISB-5-PHOBOSSHAPE-V1.0. NASA Planetary Data System. [8] Thomas P. C. (1993) *Icarus, 105,* 326-344. [9] Thomas P. and Veverka J. (1980) *Icarus, 41,* 365-380. [10] Shi X. et al. (2016) *Icarus, 43,* 12371-12379. [11] Pätzold M. et al. (2010) *Icarus, 229,* 92-98. [12] Dobrovolskis A. R. and Burns J. A. (1980) *Icarus, 42,* 422-411. [13] Willner K. et al. (2014) *PSS, 102,* 51-59.

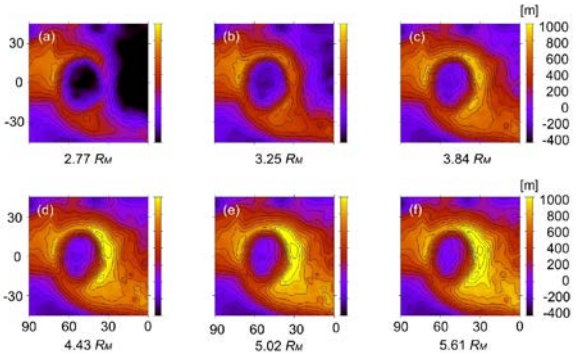

Figure 2. The dynamic height in the vicinity of Stickney crater changes as a result of a change in the orbital distance in detail.